Chapter 3

Probing the Dust and Gas in the Transitional Disk of CS Cha with *Spitzer*

Abstract: Here we present the *Spitzer* IRS spectrum of CS Cha, a member of the ∼2 Myr old Chamaeleon star–forming region, which reveals an optically thick circumstellar disk truncated at ∼43 AU, the largest hole modeled in a transitional disk to date. Within this inner hole, $\sim 5 \times 10^{-5}$ lunar masses of dust are located in a small optically thin inner region which extends from 0.1 to 1 AU. In addition, the disk of CS Cha has bigger grain sizes and more settling than the previously modeled transitional disks DM Tau, GM Aur, and CoKu Tau/4, suggesting that CS Cha is in a more advanced state of dust evolution. The *Spitzer* IRS spectrum also shows [Ne II] 12.81 μm fine-structure emission with a luminosity of 1.3×10^{29} ergs s^{-1}, indicating that optically thin gas is present in this ∼43 AU hole, in agreement with H_α measurements and a UV excess which indicate that CS Cha is still accreting 1.2×10^{-8} $M_\odot$ yr^{-1}. We do not find a correlation of the [Ne II] flux with L_X, however, there is a possible correlation with $\dot{M}$, which if confirmed would suggest that EUV fluxes due to accretion are the main agent for formation of the [Ne II] line.

3.1 Introduction

The *Spitzer Space Telescope* (Werner et al., 2004) has dramatically improved the ability to study the dust in disks by giving us detailed spectral energy distributions (SEDs) in the mid-infrared, where the dust dominates the emission. *Spitzer* Infrared Spectrograph (Houck et al., 2004) observations of T Tauri stars have provided strong evidence of dust evolution, particularly in the well surveyed ∼1-2 Myr old Taurus-Auriga star–forming region (Furlan et al., 2006). The most notable evidence of dust evolution lies in the observations of transitional disks. These disks have characteristics that fall between those objects that have clear evidence for disks and those objects with no disk material; the SEDs point to inner holes in the disk. All transitional disks have a significant deficit of flux in the near-IR which has been explained by modeling the disks with truncated optically thick disks (Uchida et al., 2004; Calvet et al., 2005b; D'Alessio et al., 2005).

CoKu Tau/4 is one of these transitional disks in Taurus (Forrest et al., 2004; D'Alessio et al., 2005). The SED of this object is photospheric below 8 μm and rises at longer wavelengths, showing weak silicate emission at 10 μm; this can be explained by the emission of the frontally illuminated edge or "wall" of an outer disk truncated at 10 AU from the star (D'Alessio et al., 2005) and the weak silicate emission arises in the atmosphere of the wall. There are no small grains in the inner disk, in agreement with CoKu Tau/4's classification as a non-accreting, weak T Tauri star. Hydrodynamical simulations indicate that this hole may be due to the formation of a planet (Quillen et al., 2004). Other studies point to photoevaporation of the disk by the star (Alexander & Armitage, 2007). However, the clearing in the

inner disk of CoKu Tau/4 is most likely due to clearing by its companion (Ireland & Kraus, 2008). Similar to CoKu Tau/4, DM Tau has been modeled with an inner disk region free of small dust and a truncated optically thick disk at 3 AU (Calvet et al., 2005b). However, this star is still accreting, indicating that gas should still remain in the inner disk region. GM Aur, which is also accreting, was modeled by Calvet et al. (2005b) with an optically thick disk truncated at 24 AU and a small amount of dust in the inner disk which leads to its observed near-IR excess. This disk hole could also be due to a planet (Rice et al., 2003). TW Hya, a transitional disk in the ∼10 Myr old TW Hya association (Jayawardhana et al., 1999; Webb et al., 1999), has an outer optically thick disk with a 4 AU hole filled with an inner optically thin region populated by a small amount of dust (Calvet et al., 2002; Uchida et al., 2004).

Not only has *Spitzer* been a powerful tool in exploring the dust evolution in circumstellar disks, it also has the potential to access new probes of the gas evolution in these disks, an area of study which is still in its infancy and largely uncertain. High-resolution molecular spectroscopy has permitted us to access abundant molecular tracers within the inner disk such as H_2 and CO (Bergin et al., 2004; Najita et al., 2007b). A new gas diagnostic has emerged in the mid-infrared with the detection of [Ne II] emission with *Spitzer*. [Ne II] emission at 12.81 μm has been detected from a few T Tauri stars that were observed as part of the FEPS *Spitzer* Legacy program (Pascucci et al., 2007) as well as in the transitional disks CS Cha, DM Tau, and TW Hya (Espaillat et al., 2007a).

We will present and analyze *Spitzer* IRS data of CS Cha, a transitional disk in the ∼2 Myr old Chamaeleon star–forming region (Luhman, 2004).

3.2 Observations

CS Cha was observed by the *Spitzer* IRS instrument on 11 July 2005 in Staring Mode (AOR ID: 12695808). We used the short- and long-wavelength, low-resolution (SL, LL) modules of IRS at a resolving power of $\lambda/\delta\lambda = 60 - 100$. The total exposure time was 28 and 12 seconds for SL and LL respectively. We reduced the data with the SMART package (Higdon et al., 2004). We follow the same reduction procedure as Calvet et al. (2005b). The 12.81 μm [Ne II] line is not extended and is consistent with the CS Cha point source.

The photometry at 24 and 70 μm was extracted from the MIPS post-BCD mosaicked images (AOR ID: 3962112) using the aperture photometry routine in the Astronomical Point Source Extraction (APEX) software package developed by the SSC (Makovoz & Marleau, 2005). An aperture of radius 14.″94, with a sky annulus between 29.″88and 42.″33, was used at 24 μm while an aperture of radius 29.″55, with a sky annulus between 39.″40 and 68.″95, was used at 70 μm. Both fluxes were aperture corrected by factors of 1.143 at 24 μm and 1.298 at 70 μm, as calculated by Su et al. (2006). No color correction was applied.

3.3 Analysis

3.3.1 Dust Properties

Figure 3.1 shows the SED of CS Cha consisting of optical (Gauvin & Strom, 1992), 2MASS, L-band (Luhman, 2004), *Spitzer* IRS, IRAS (Gauvin & Strom, 1992), MIPS, and millimeter (Henning et al., 1993) data. We also show the median SED of Taurus (D'Alessio et al., 1999; Furlan et al., 2006) which emphasizes the stark deficit of flux

in the near infrared, an indicator of an inner disk hole, which is characteristic of transitional disks.

A distance of 160 pc to Chamaeleon I (Whittet et al., 1997) and a spectral type of K6 from Luhman (2004) are adopted. The extinction is calculated by fitting the observed photospheric colors to the photosphere calibrated by a standard K6 star with an effective temperature of 4205 K (Kenyon & Hartmann, 1995). Data are then dereddened with an A_V of 0.8 and the Mathis (1990) reddening law. Stellar parameters (M_*, R_*, L_*) are listed in Table 3.1; the mass was derived from the Siess et al. evolutionary tracks (Siess et al., 2000). An inclination angle of 60° to the line of sight is adopted.

The SED suggests a UV excess which is thought to be formed in the accretion shock on the stellar surface (Calvet & Gullbring, 1998). This is supported by H_α equivalent widths of 20 Å (Luhman, 2004) and 65 Å (Hartigan, 1993), which indicate CS Cha is accreting (White & Basri, 2003). We calculate a mass accretion rate of 1.2×10^{-8} $M_\odot$ yr^{-1} from this U-band excess following Gullbring et al. (1998), with a typical uncertainty of a factor of 2 or 3 (Calvet et al., 2004).

We model CS Cha as a truncated optically thick disk with a frontally illuminated vertical wall and an inner optically thin region. The black solid line in Figure 3.2 is the best fit model to the observations; different model components are represented by the broken lines. We use a grain-size distribution that follows a power-law of the form $a^{-3.5}$, where a is the grain radius, with a_{min} of 0.005 μm and a_{max} of 5 μm. The structure and emission of the optically thick disk (Figure 3.2) is calculated with models including dust settling following D'Alessio et al. (2006), where we use

millimeter fluxes (Henning et al., 1993; Lommen et al., 2007) and MIPS to constrain the outer disk properties. Input parameters are the stellar properties and the mass accretion rate of the disk ($\dot{M}$), the viscosity parameter (α), the dust composition, and the settling parameter $\epsilon = \zeta_{up}/\zeta_{st}$, i.e. the mass fraction of the small grains in the upper layers relative to the standard dust-to-gas mass ratio (D'Alessio et al., 2006). Table 3.1 shows all relevant values. The disk mass, 0.04 $M_\odot$, is determined by the mass surface density which is proportional to $\dot{M}/\alpha$ and the assumed disk radius. This result is not inconsistent with the disk mass of 0.021 $M_\odot$ derived by Henning et al. (1993) from 1.3 mm fluxes.

The optically thick disk has an edge or "wall" directly exposed to stellar radiation (Figure 3.2). The radiative transfer in the wall atmosphere is calculated following D'Alessio et al. (2005) with the following inputs: stellar mass (M_*), stellar radius (R_*), $\dot{M}$, stellar effective temperature (T_*), maximum and minimum grains sizes, temperature of the optically thin wall atmosphere (T_{wall}). See Table 3.1 for the wall's location (R_{wall}), maximum grain size (a_{max}), and other parameters.

The emission at 10 μm comes from the optically thin inner region (Calvet et al., 2005b) which extends up to 1 AU from the star and has a minimum grain size of 1.9 μm and a maximum grain size of 2.1 μm (Figure 3.2). The total emission is scaled to the vertical optical depth at 10 μm, $\tau_0 \sim 0.009$. This region is populated by $\sim 10^{-12}$ $M_\odot$ or $\sim 5\times10^{-5}$ M_{moon} of uniformly distributed dust. This small amount of dust leads to the slight 5 – 8 μm excess above the photosphere (most easily seen in Figure 3.3). The dust in this region is composed of 88% amorphous silicates, 5% of amorphous carbon, 5% organics, 1% troilite and less than 1% of enstatite and

forsterite.

Figure 3.3 illustrates the necessity of larger grains in both the wall and optically thin inner region to fit the observations. The solid line corresponds to the model of the wall and optically thin region with the larger grain sizes which we adopted above. The dotted line corresponds to models with the smaller, ISM-like grains, as are found in the Taurus transitional disks CoKu Tau/4, DM Tau, and GM Aur. Figure 3.3 shows that larger grains have better agreement with the slope of the SED beyond 15 μm and are necessary to produce the slight near-infrared excess, the shape of the 10 μm feature, and the >20 μm IRS emission in CS Cha.

3.3.2 Gas Properties

We detect [Ne II] fine-structure emission at 12.81 μm ($^2P_{1/2} \rightarrow^2 P_{3/2}$) in CS Cha (see Figure 3.3). Using the IRAF tool *SPLOT*, we find the integrated line flux, $\int F_\lambda d\lambda$, to be 4.3$\pm$0.6 $\times$ 10^{-14} ergs cm^{-2} s^{-1} or 1.3 $\times$ 10^{29} ergs s^{-1}.

Glassgold et al. (2007) have recently suggested that circumstellar disks exposed to stellar X-rays would produce [Ne II] fine-structure emission at a level that would be detectable with *Spitzer* in nearby star–forming regions. In the Glassgold et al. (2007) model, the disk surface is both ionized and heated by stellar X-rays. Ne ions (primarily Ne^+ and Ne^{2+}) are produced through X-ray ionization and destroyed by charge exchange with atomic hydrogen and radiative recombination. Alternatively, (Gorti & Hollenbach, 2009) propose that EUV photons from the stellar chromosphere and/or stellar accretion can create an ionized HII-region-like layer at the disk surface that can also produce significant [Ne II] emission.

3.4 Discussion & Conclusions

CS Cha shows clear evidence of advanced dust evolution in relation to other transitional disks: it has significant grain growth and substantial settling in its outer disk. The dust in the wall of the outer disk in CS Cha has grown to much larger sizes (5 μm) than the dust in the transitional disks CoKu Tau/4, DM Tau, GM Aur, and TW Hya, all of which have maximum grain sizes in the outer wall of 0.25 μm (D'Alessio et al., 2005; Calvet et al., 2005b, 2002; Uchida et al., 2004), and CS Cha has large grains in the inner optically thin region as well, similar to TW Hya (Sargent et al., 2006). CS Cha also needs more settling in the outer disk ($\epsilon = 0.01$) to fit the far-infrared and millimeter data, indicating much higher dust depletion in the upper layers than found in GM Aur and DM Tau, which were modeled with $\epsilon = 0.1$ and 0.5, respectively (Calvet et al., 2005b; Hughes et al., 2009) . In addition, CS Cha further stands out due to its large hole size, having the largest modeled to date at $\sim$ 43 AU. This large inner hole serves to decrease the mid-infrared dust continuum and hence increase the line to continuum ratio, facilitating the detection of [Ne II] fine-structure emission.

The luminosity of the [Ne II] 12.81 μm line in CS Cha is strong compared to other [Ne II] detections in disks. The luminosity seen in DM Tau is 1.3×10^{28} ergs s^{-1} and for GM Aur the 5 σ upper limit is 7.4×10^{28} ergs s^{-1} (measured from spectra in Calvet et al., 2005b). TW Hya shows [Ne II] emission at 12.81 μm with a luminosity of 3.9×10^{28} ergs s^{-1} (measured from Uchida et al., 2004). In addition, the luminosities seen in four CTTS that were observed in the FEPS survey are $\sim 10^{28}$ ergs s^{-1} (Pascucci et al., 2007).

To gain insight into the origin of the Neon emission we compare $L_{[NeII]}$ to L_X and $\dot{M}$ in Figure 3.4. We see no apparent correlation between $L_{[NeII]}$ and L_X as was reported by Pascucci et al. (2007) and as would be expected from the X-ray heating model of Glassgold et al. (2007), which suggests that other processes like viscous heating, jets, and UV heating are involved (Glassgold et al., 2007). We find a possible correlation between $L_{[NeII]}$ and $\dot{M}$ which suggests that accretion related heating may play a substantial role in producing [Ne II] emission. Accretion related processes that affect the disk heating are viscous dissipation and irradiation by UV emission from the accretion shock region. Calvet et al. (2004) show that FUV fluxes scale with L_{acc}, and a similar scaling is expected for the EUV; in turn, Gorti & Hollenbach (2009) show that EUV heating and ionization can result in significant [Ne II] emission.

Nevertheless, both the X-ray and EUV heating models under-predict the $L_{[NeII]}$ seen in CS Cha (Glassgold et al., 2007; Pascucci et al., 2007). We note that the optically thin inner region of CS Cha is populated by large grains, which would favor UV flux penetration of the gas (Aikawa & Nomura, 2006) and possibly lead to enhanced $L_{[NeII]}$. Further exploration of the gas and dust in other transitional disks is necessary to test any link between these components. Similarly, jets and outflows, which are also characteristic of sources with higher accretion rates, may contribute to a positive trend. High resolution spectroscopy of CS Cha can explore this contribution from the jet (Takami et al., 2003).

Table 3.1. Stellar and Model Properties of CS Cha

Stellar Parameters	
M_* ($M_\odot$).....	0.91
R_* ($R_\odot$).....	2.3
T_* (K).....	4205
L_* ($L_\odot$).....	1.5
$\dot{M}$ ($M_\odot$ yr^{-1}).....	1.2×10^{-8}
Distance (pc).....	160
A_V.....	0.8
Wall Parameters	
R_{wall} (AU).....	42.7
a_{min} (μm).....	0.005
a_{max} (μm).....	5
T_{wall} (K).....	90
z_{wall} (AU)[1].....	5
Optically Thick Outer Disk Parameters	
$R_{d,out}$ (AU).....	300
ϵ.....	0.01
α.....	0.005
M_d ($M_\odot$).....	0.04
Optically Thin Inner Region Parameters	
$R_{in,thin}$ (AU).....	0.1
$R_{out,thin}$ (AU).....	1
$a_{min,thin}$ (μm).....	1.9
$a_{max,thin}$ (μm).....	2.1
$M_{d,thin}$ ($M_\odot$).....	1.7×10^{-12}

[1] z_{wall} is the height above the disk midplane

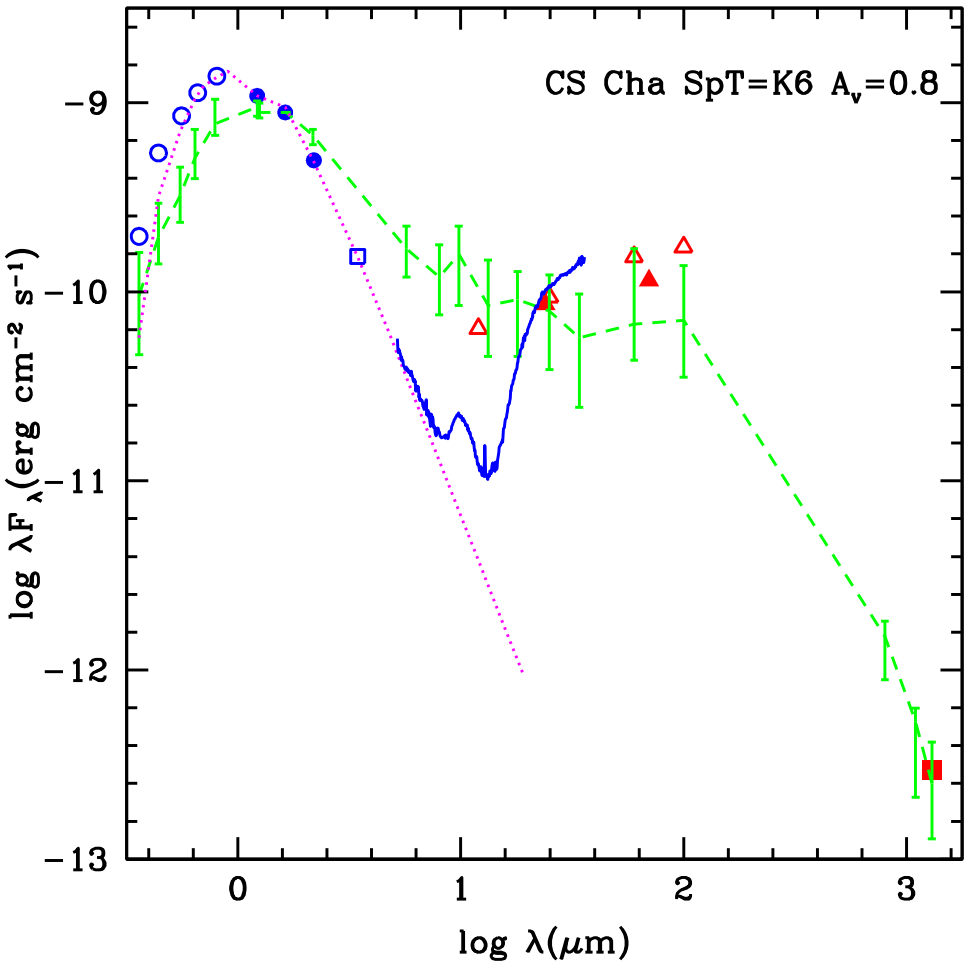

Figure 3.1 SED of CS Cha. Optical (open circles), J,H,K (filled circles), L-band (open square), *Spitzer* IRS data (blue solid line), IRAS (open triangles), MIPS (closed triangles) and sub-mm (closed square) are shown. Red corresponds to observed magnitudes and blue symbols are dereddened magnitudes. The short-dashed green line with quartiles is the median SED of Taurus and the dotted magenta line is the stellar photosphere.

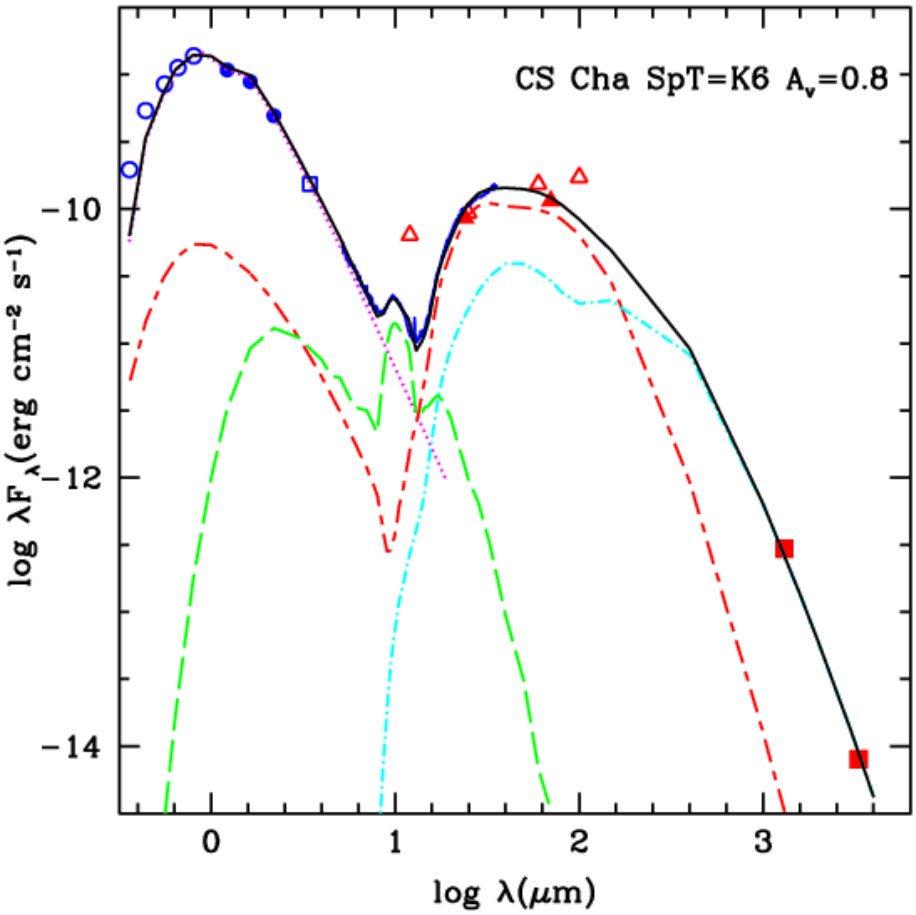

Figure 3.2 SED and transitional disk model of CS Cha. The solid black line is the best fit model with parameters from Table 3.1. Separate model components are also shown: wall (scattered and thermal emission; red short-long-dash line), optically thick disk (blue dot-dash), optically thin inner region (green long-dashed), stellar photosphere (magenta dotted line). Note that the model does not fit the IRAS points. IRAS has a larger field of view than *Spitzer* which could overreport the flux, especially at 100 μm. However, the model agrees with the MIPS data, which has a smaller field of view than IRAS. We also include ATCA 3.3 mm data (Lommen et al., 2007).

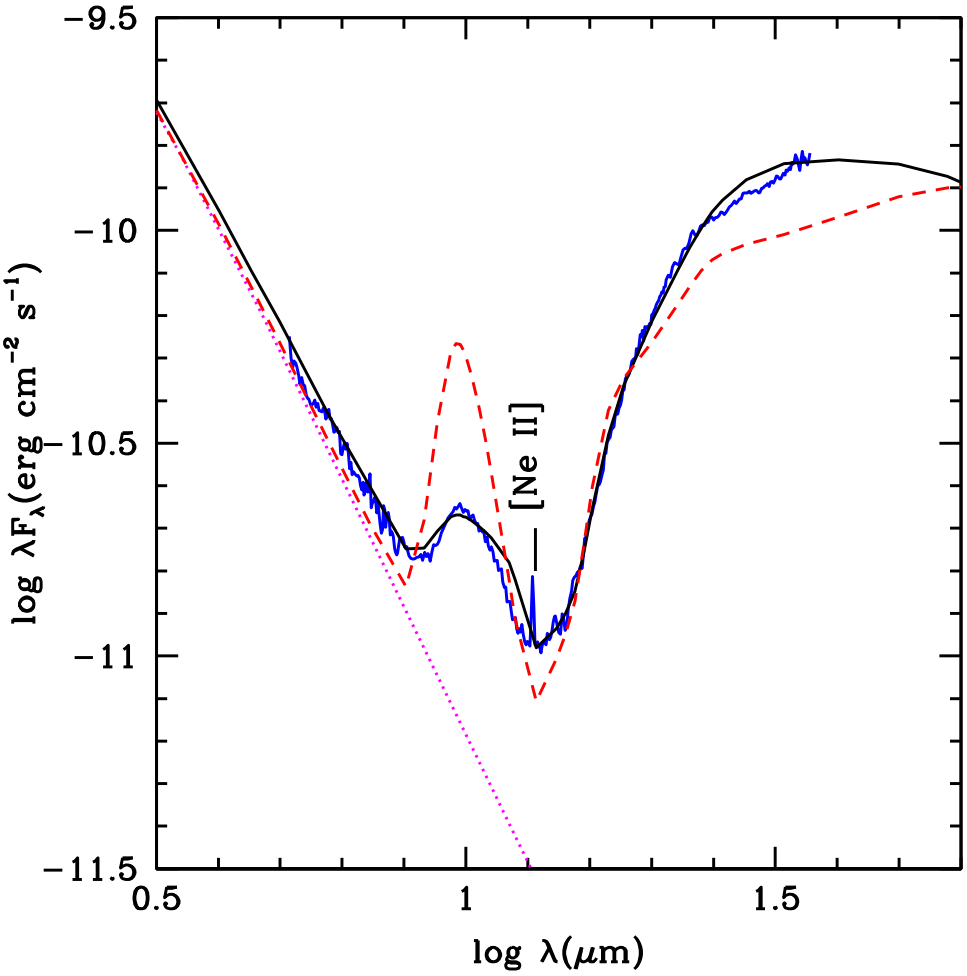

Figure 3.3 Models of CS Cha with big grains versus small grains. The solid black line corresponds to the model that uses big grains and it is the best-fit disk model shown in Figure 3.2 and Table 3.1. The red dashed line is the model that uses small grains; the wall has a_{max}=0.25 μm and the optically thin region has a_{min}=0.005 μm and a_{max}=0.25 μm.

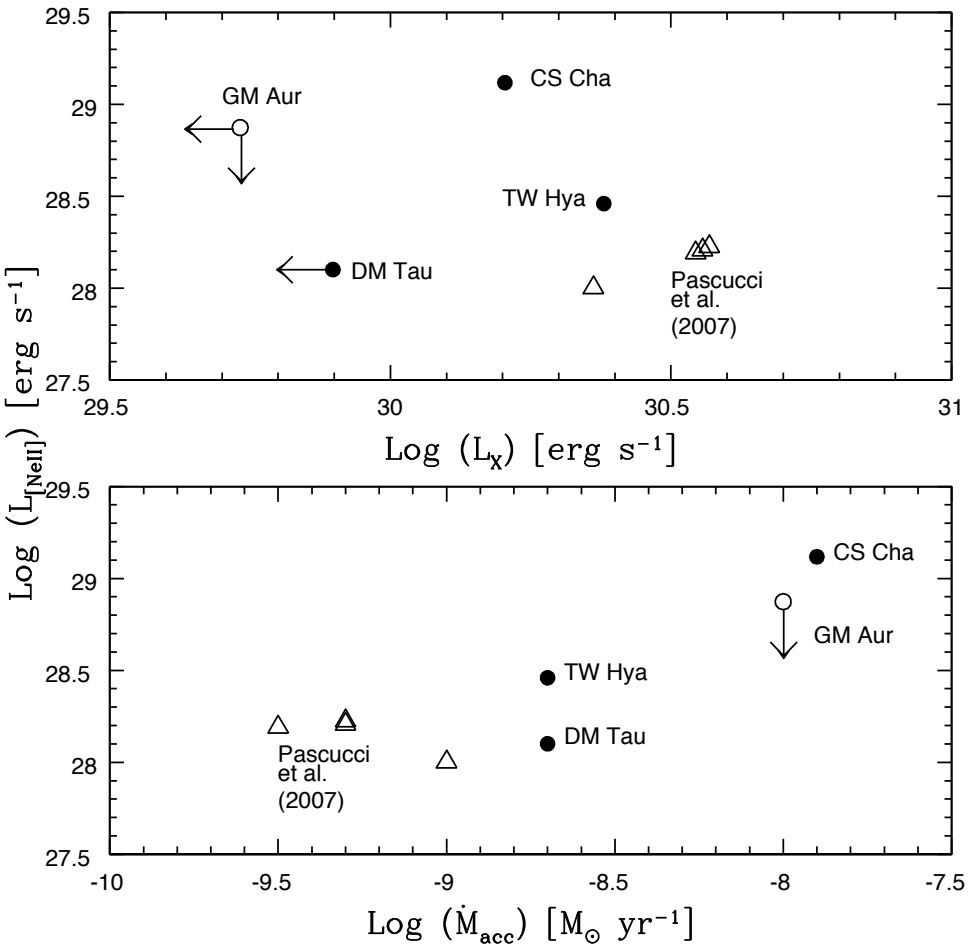

Figure 3.4 Comparison of $L_{[NeII]}$ with L_X and $\dot{M}$ for TTS. Top: $L_{[NeII]}$ vs. L_X. There is no obvious correlation. Triangles are from Pascucci et al. (2007), circles correspond to [Ne II] luminosities derived in this chapter. The L_X for CS Cha and TW Hya are from Feigelson et al. (1993) and Kastner et al. (1999), scaled to 160 and 55 pc, respectively. We show upper limits for the $L_{[NeII]}$ of GM Aur and the L_X of GM Aur and DM Tau (Neuhaeuser et al., 1995). All L_X are from ROSAT and vary by a factor of $\sim$2. Bottom: $L_{[NeII]}$ vs. $\dot{M}$. There is a possible positive correlation. The $\dot{M}$ for CS Cha is derived here and $\dot{M}$ for GM Aur and DM Tau are from Calvet et al. (2005b). TW Hya's $\dot{M}$ is from veiling measurements but varies between 0.4×10^{-9} to 10^{-8} $M_\odot$ yr^{-1} (Alencar & Batalha, 2002; Muzerolle et al., 2000).